CORROSION SCIENCE AND TECHNOLOGY, Vol.5, No.4(2006), pp.141~148

Effects of Film Formation Conditions on the Chemical Composition and the Semiconducting Properties of the Passive Film on Alloy 690

HeeJin Jang and †HyukSang Kwon

Dept. of Materials Science and Engineering, Korea Advanced Institute of Science and Technology
373-1 GuSeongDong, YuSeongGu, DaeJeon, 305-701, Republic of Korea

The chemical composition and the semiconducting properties of the passive films formed on Alloy 690 in various film formation conditions were investigated by XPS, photocurrent measurement, and Mott-Schottky analysis.

The XPS and photocurrent spectra showed that the passive films formed on Alloy 690 in pH 8.5 buffer solution at ambient temperature, in air at 400 ℃, and in PWR condition comprise Cr_2O_3, $Cr(OH)_3$, γ-Fe_2O_3, NiO, and $Ni(OH)_2$. The thermally grown oxide in air and the passive film formed at high potential (0.3 V_{SCE}) in pH 8.5 buffer solution were highly Cr-enriched, whereas the films formed in PWR condition and that formed at low potential (-0.3 V_{SCE}) in pH 8.5 buffer solution showed relatively high Ni content and low Cr content. The Mott-Schottky plots exhibited n-type semiconductivity, inferring that the semiconducting properties of the passive films formed on Alloy 690 in various film formation conditions are dominated by Cr-substituted γ-Fe_2O_3. The donor density, i.e., concentration of oxygen vacancy, was measured to be 1.2×10^{21}~4.6×10^{21} cm^{-3} and lowered with increase in the Cr content in the passive film.

Keywords *: alloy 690; passive film; photocurrent; mott-schottky analysis; point defects.*

1. Introduction

Ni based alloys are widely used in many industrial facilities which requires superior corrosion resistance even to stainless steels. Particularly, Alloy 690 is recently employed as a steam generator tube material in nuclear power plants replacing Alloy 600, due to its excellent resistance to corrosion, especially to stress corrosion cracking (SCC). The corrosion resistance of alloys is largely dependent on the protective passive film formed on the surface. Since the protectiveness of passive film is associated with its structure, composition, and semiconducting properties,[1)-3)] elucidating the nature of the passive film on the alloys is a prerequisite for understanding such an excellent corrosion resistance of Alloy 690.

Generally, the higher Cr content in the alloy or in the passive film is known to be responsible for the better corrosion resistance of Ni based alloys.[4)-6)] It is reported that the stability of the passive film of Alloy 600 is improved by increasing Cr concentration in the film by potential cycling.[4)] SCC susceptibility of Ni-Cr-Fe alloys is low for the alloy with high Cr content[5)] or that with the passive film highly enriched with Cr oxide.[6)] Otherwise, some authors explained the corrosion resistance of alloys in terms of the semiconducting properties of the passive film.[3),7)] Hur[7)] proposed that the semiconducting type of the passive film on the alloy contributes the corrosion resistance of Alloy 600 and Alloy 690 as well as the Cr content. The passive film of Alloy 600 exhibited n-type and p-type behavior at high and low potential regions, respectively, while that of Alloy 690 showed only n-type behavior in the Mott-Schottky plots in 10 % NaOH solution at 315 ℃. He explained based on the Point Defect Model[8)] that the passive film of Alloy 690 is more protective than that of Alloy 600 because the n-type film is dominated by oxygen vacancy, which leads to film growth and inhibits dissolution of metal ion. On the other hand, p-type passive film with high concentration of cation vacancy easily becomes unstable since metallic ions move readily to the film/solution interface and dissolve in solution. Sato[3)] also suggested that n-type passive film has better protectiveness than p-type film by study on transport behavior of ions through the oxide. Further, the stability of the passive film is significantly affected not only by the type of the vacancy but also by the concentration of vacancy in that the flux of vacancy plays an important role in growth and breakdown of the passive film.[8)-9)]

As mentioned above, both of the chemical composition

†Corresponding author: hskwon@kaist.ac.kr

and the semiconducting properties of passive film determine the corrosion resistance of alloys.[4)-6)] We can suppose that different chemical composition of the passive film should involve certain change of the defect property of the film and consequently bring improvement or degradation of the corrosion resistance of Ni-based alloys. The objective of this study is to examine the chemical composition and the semiconducting properties, especially the density of defect, of the passive films formed on Alloy 690 in various film formation conditions and to find the correlation between them.

2. Experimental procedure

Alloy 690, a commercially produced pipe of 1.09 mm thickness and 19.05 mm outer diameter, was used in this study. Specimens were machined from the tube and flattened into a sheet form by press. The chemical composition of the alloy is shown in Table 1. All samples were subjected to an isothermal solution annealing at 1150 ℃ for 1 h, followed by a water quench, and then aged at 700 ℃ for 15 h. The working electrodes were mounted in an epoxy resin with an exposed area of 0.2 cm^2.

A conventional three-electrode cell of 1 L-multi neck flask was used for the electrochemical film formation and tests. The cell was equipped with a platinum counter electrode and a saturated calomel reference electrode (SCE). All the electrode potentials are referred to the SCE. The photocurrent measurement and Mott-Schottky analysis were carried out in deaerated buffer solution (pH = 8.5). The buffer solution was made of H_3BO_3, $C_6H_8O_7 \cdot H_2O$, and $Na_3PO_4 \cdot 12H_2O$.

The passive films were formed by the following 4 kinds of formation methods:

- Applying 0.3 V_{SCE} for more than 24 h in pH 8.5 buffer solution at ambient temperature after cathodic cleaning at -1.0 V_{SCE} for 5 min.
- Applying -0.3 V_{SCE} for more than 24 h in pH 8.5 buffer solution at ambient temperature after cathodic cleaning at -1.0 V_{SCE} for 5 min.
- Exposing in air at 400 ℃ for 2 h.
- Exposing in a pressurized water reactor (PWR) simulated condition for 60 days.

The PWR simulated condition in this study means 325 ℃ water with 1200 ppm of B, 2 ppm of Li, and 45 cc/kg of dissolved hydrogen. Dissolved oxygen was less than 5 ppb, and the pH was 5.8.

Table 1. Chemical compositions of alloy 690 used in this study (wt.%)

	C	Si	Mn	S	Al	Co	Cr	Cu	Fe	Ni	Ti
Alloy 690	0.014	0.28	0.26	0.0030	0.02	0.01	30.43	0.03	9.54	59.18	0.20

After film formation, the composition and semiconducting properties of the passive film were analyzed by XPS, photocurrent measurement, and Mott-Schottky analysis. Photocurrent spectra for the passive films were measured at an applied potential (U_{app}) with continuous illumination condition. A 300 W Xenon arc lamp was used as a light source and a monochromatic light with wavelength of 200 ~ 800 nm was provided by a scanning digital monochromator controlled by a stepping motor at a scan rate of 1 nm/s. Details in the photocurrent measuring system were described elsewhere.[10)-11)] For Mott-Schottky analysis, the capacitance was measured with sweeping the applied potential at a rate of -1 mV/s. The excitation voltage was 10 mV (peak-to-peak) and the frequency was 1 kHz. PHI 5800 ESCA System with Al Kα anode (350 W, 15 kV) was used for XPS analysis. The reference energies were the C1s signal at 284.5 eV and the O1s signal at 531.0 eV. In-depth composition profiling of passive film was performed using Ar ion gun (base pressure = 2×10^{-10} torr, working pressure = 2×10^{-8} torr, energy: 3 ~ 4 kV). The sputter rate was calibrated with SiO_2.

3. Results and discussion

3.1 Potentiodynamic polarization response

Fig. 1 shows the potentiodynamic polarization response of Alloy 690 in pH 8.5 buffer solution. The corrosion potential of the alloy was measured to be -0.7 V_{SCE} and its passive region extended from the corrosion potential to about 0.3 V_{SCE}. The increase in current density at 0.3

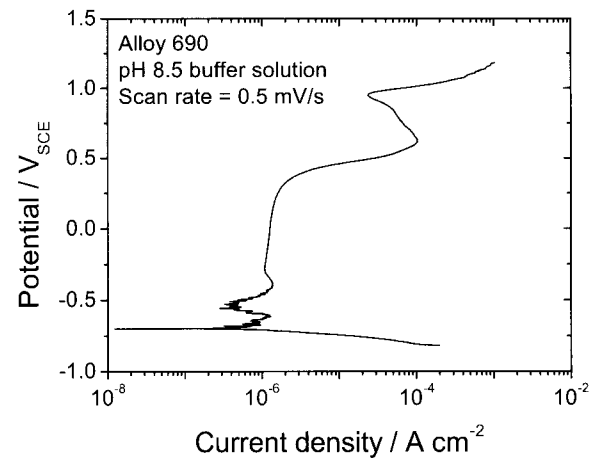

Fig. 1. Potentiodynamic polarization curve for Alloy 690 in pH 8.5 buffer solution at ambient temperature, measured at a potential scan rate of 0.5 mV/s.

V_{SCE} is due to transpassive oxidation of Cr^{3+} to Cr^{6-}, and that at 1.0 V_{SCE} is associated with oxygen evolution reaction on the passive film. The decrease in current density at the potential between 0.5 V_{SCE} and 1.0 V_{SCE} is due probably to an unstable secondary passivation by Fe and Ni. Based on the passive region in the polarization curve in Fig. 1, both 0.3 V_{SCE} and -0.3 V_{SCE} were selected as the film formation potentials (U_f) for examining the effects of film formation potential on the properties of passive films.

3.2 XPS analysis

The depth profile for the concentration of Ni, Cr, and Fe in the passive film formed on Alloy 690 in various film formation conditions are shown in Fig. 2. The thickness of the passive film formed in pH 8.5 buffer solution at ambient temperature appeared to be about 2 ~ 4 nm and was increased by increasing film formation potential (Figs. 2(a) and (b)). The thickness of the oxide films formed in air at 400 ℃ and in the simulated PWR condition were about 30 nm and 50 nm, respectively (Figs. 2(c) and (d)). For the passive films formed in pH 8.5 buffer solution at ambient temperature (Figs. 2(a) and (b)), Cr was most enriched at the surface of the passive film and its concentration was gradually decreased with depth. From the depth profiles for the passive films formed at high temperatures (Figs. 2(c) and (d)), the concentration of Cr exhibited the maximum at the midst of the passive film where the concentration of Ni showed the minimum.

The passive film formed on Alloy 690 at 0.3 V_{SCE} in pH 8.5 buffer solution and that in air at 400 ℃ appeared mostly composed of Cr-rich oxide. In contrast, the concentrations of Ni and Cr were comparable in the passive film formed at -0.3 V_{SCE} in buffer solution. Cr content was higher than Ni only at the inner part of the film formed in the simulated PWR condition. Fe content in the passive film was similar to or lower than that in the alloy except for the film formed in PWR condition in which the

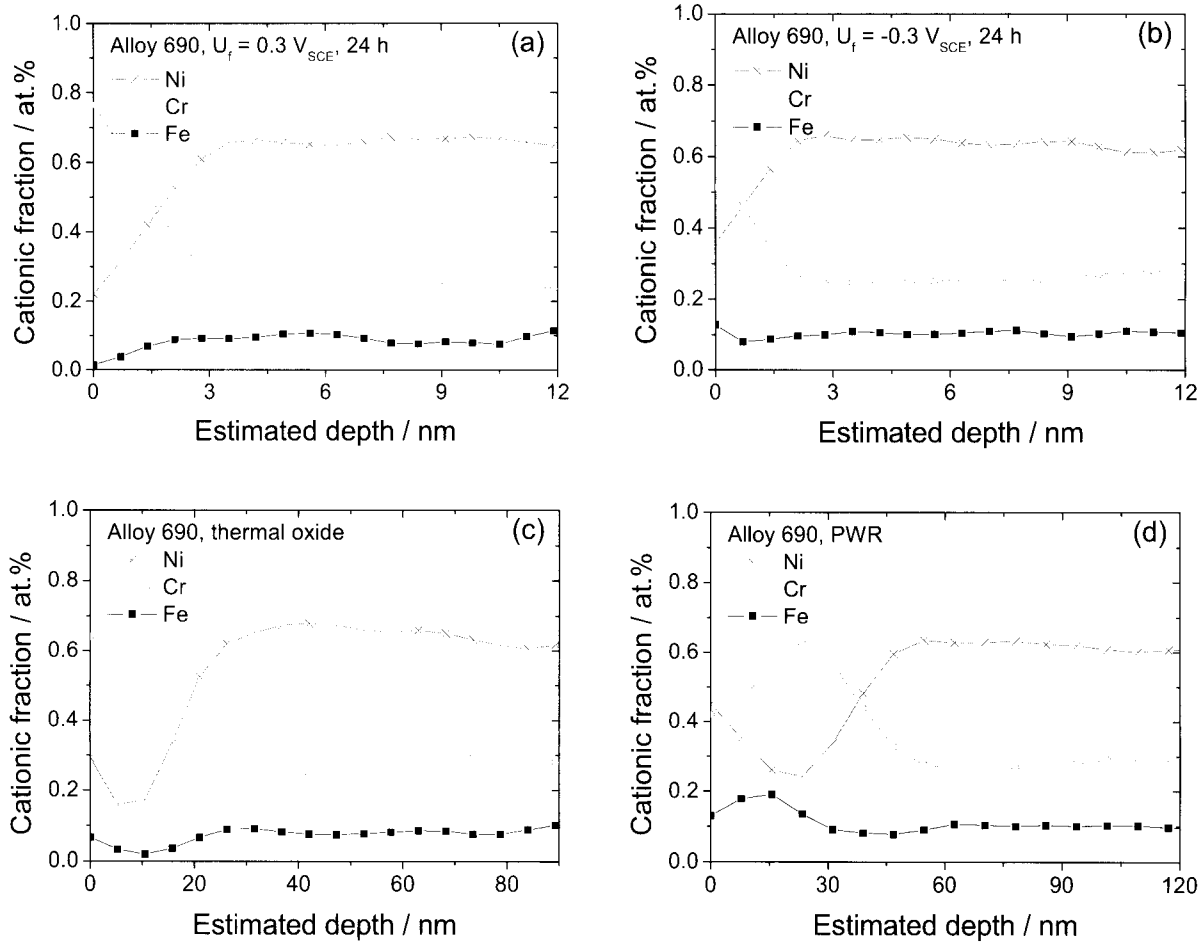

Fig. 2. XPS concentration depth profiles for the passive films formed on Alloy 690 (a) at 0.3 V_{SCE}, (b) at -0.3 V_{SCE} for 24 h in pH 8.5 buffer solution at ambient temperature, (c) in air at 400 ℃ for 2 h, and (d) in PWR simulated condition for 60 days.

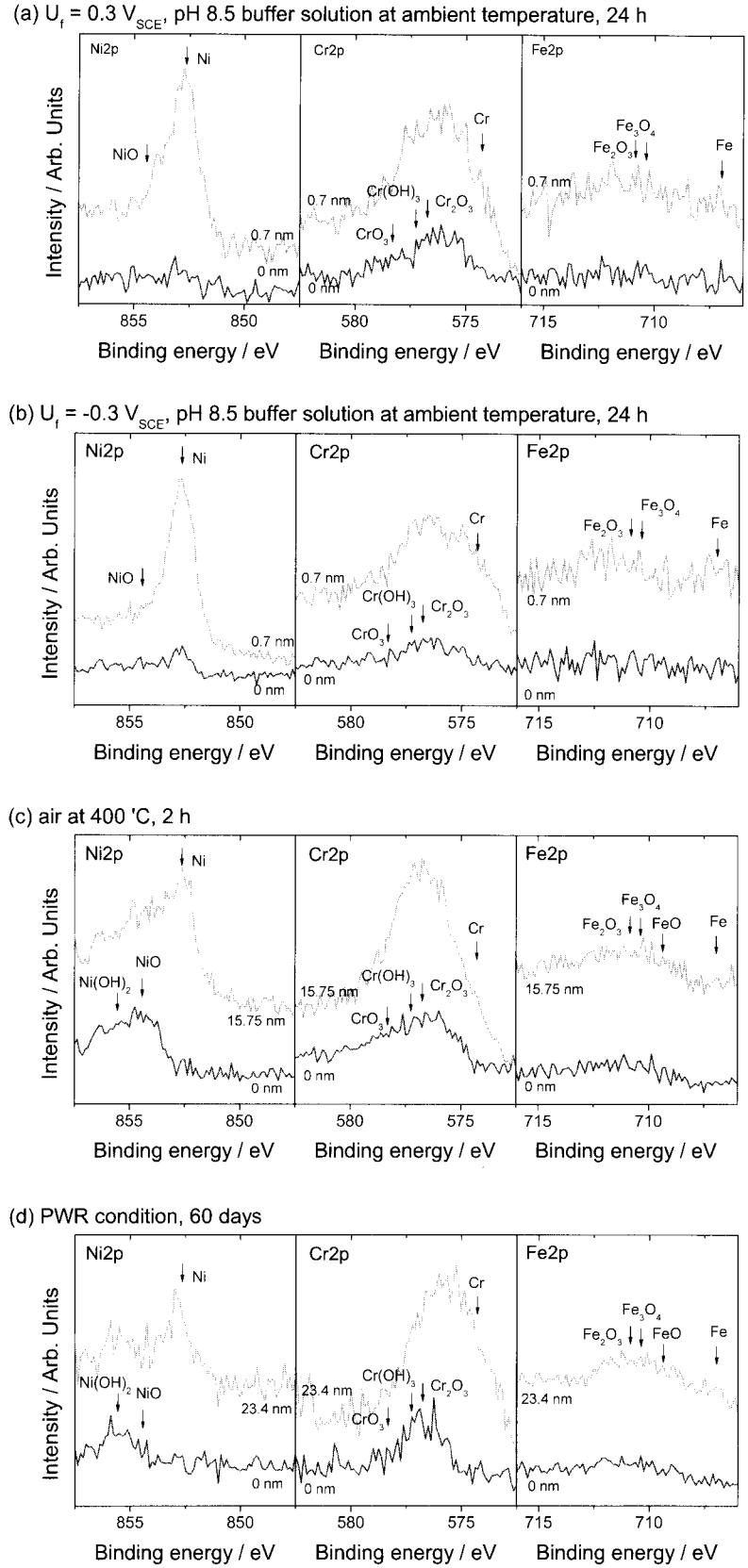

Fig. 3. XPS high resolution spectra of Ni, Cr, and Fe with sputtering depth for the passive film formed on Alloy 690 (a) at 0.3 V_{SCE}, (b) at -0.3 V_{SCE} in pH 8.5 buffer solution at ambient temperature, (c) in air at 400 ℃, and (d) in PWR condition.

Table 2. Binding energies (eV)[12] for chemical states referred in Fig. 3.

Ni2p	Ni	Ni^{2+} (NiO)	Ni^{2+} ($Ni(OH)_2$)	
	852.7	854.3	852.7	
Cr2p	Cr	Cr^{3+} (Cr_2O_3)	Cr^{3+} ($Cr(OH)_3$)	Cr^{6+} (CrO_3)
	574.3	576.8	577.4	578.3
Fe2p	Fe	Fe^{3+} (Fe_2O_3)	Fe^{3+} or Fe^{2+} (Fe_3O_4)	Fe^{2+} (FeO)
	707.0	710.9	710.4	709.4

concentration of Fe was about twice in the film as that in the alloy.

The XPS high resolution spectra (Fig. 3) of Ni, Cr, and Fe for the passive films formed on Alloy 690 demonstrated that various oxides containing Ni^{2+}, Cr^{3+}, Cr^{6+}, Fe^{2+}, and Fe^{3+} as well as hydroxides of Ni^{2+} and Cr^{3+} are present in the passive films. The spectral intensity of each element varied depending on the film formation conditions and sputtering depth. Ni and Fe oxides were hardly found from the XPS spectra for the passive films formed in pH 8.5 buffer solution at ambient temperature (Figs. 3(a) and (b)) due to the small amount of these oxides as well as the small thickness of the films. For the passive films formed at 0.3 V_{SCE} at which Cr-transpassive dissolution begins to occur (Fig. 1), evidence of Cr^{6+} was observed (Fig. 3(a)) while it was not detected for the film formed at -0.3 V_{SCE} (Fig. 3 (b)). Both NiO and $Ni(OH)_2$ was considered to exist in the film formed in air at 400 °C (Fig. 3(c)). But Ni^{2+} in the film formed in PWR condition was mostly in hydroxide form (Fig. 3(d)). For the passive film formed in PWR condition, Cr was mainly in form of Cr^{3+} (Fig. 3(d)) unlike the thermal oxide in which Cr^{3+} and Cr^{6+} coexisted (Fig. 3(c)). Fe oxides with Fe^{2+} and Fe^{3+} appeared to be present in the passive film formed in air and in PWR condition, from Figs. 3(c) and (d).

3.3 Photocurrent response

Photocurrent spectra for the passive films were measured to analyze the structure and the composition of the films formed in various film formation conditions. Fig. 4(a) shows the photocurrent response of the passive film formed on Alloy 690 at -0.3 V_{SCE}. The photocurrent spectrum is separated into three components with peaks at about 3.7, 4.5, and 5.8 eV, respectively. From the previous study,[11] the passive film of Ni is suggested to be composed of outer $Ni(OH)_2$ and inner NiO layers which induce photocurrent peaks at 4.5 eV and 5.7 eV, respectively. For the passive film of Cr,[13] two photocurrent

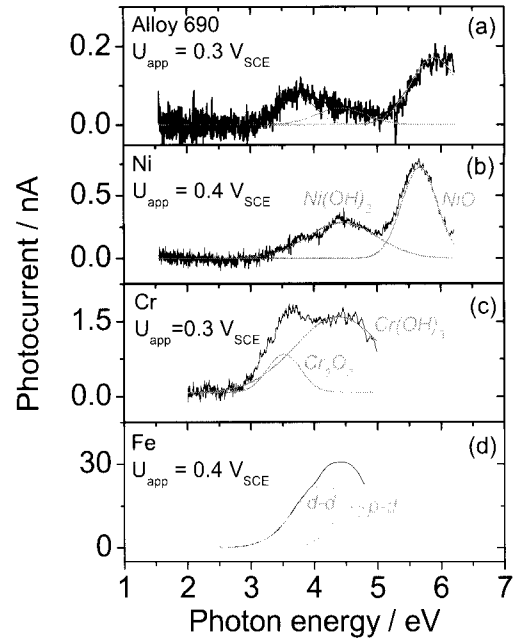

Fig. 4. Photocurrent spectra for the passive film formed on (a) Alloy 690, (b) Ni,[11] (c) Cr,[13] and (d) Fe[14] measured in pH 8.5 buffer solution.

spectral components with peaks at 3.6 eV and 4.7 eV were measured and attributed to Cr_2O_3 and $Cr(OH)_3$, respectively. It was reported that the passive film of Fe consists of γ-Fe_2O_3 involving d-d ($Fe^{2+} \rightarrow Fe^{3+}$) and p-d (O2p $\rightarrow$ Fe3d) electron transitions.[14] Cho et al.[10] suggested that the passive films of Fe-(5 ~ 20)Cr alloys are composed of Cr-substituted γ-Fe_2O_3, based on the photocurrent spectra with peaks at the same positions but with much low intensity compared with the spectrum for the film on pure Fe. Comparing the photocurrent spectrum for the passive film of Alloy 690 with those of Ni, Cr, and Fe, the peak at about 3.7 eV in Fig. 4(a) is obviously originated from Cr_2O_3. The photocurrent component with peak at 4.5 eV can be associated with $Ni(OH)_2$, $Cr(OH)_3$, and also Cr-substituted γ-Fe_2O_3. The photocurrent peak at 5.8 eV evidently originated from NiO. Cr^{6+} in the passive film did not generate any additional photocurrent peak presumably because it is incorporated in Cr-substituted γ-Fe_2O_3[10] without forming its own oxide phase.

The photocurrent spectra (Fig. 5) for the passive films formed on Alloy 690 in various film formation conditions exhibited the spectral components with peaks at about 3.7, 4.5, and 5.7 eV, associated with Cr_2O_3, $Cr(OH)_3$, Fe_2O_3, $Ni(OH)_2$, and NiO. In Fig. 5, the applied potentials were selected to recognize all of the photocurrent peaks for each passive film, considering the intensity and the sign of each photocurrent component in the spectra are varied with the applied potential.[11),15),16] Besides, intensity and sign of

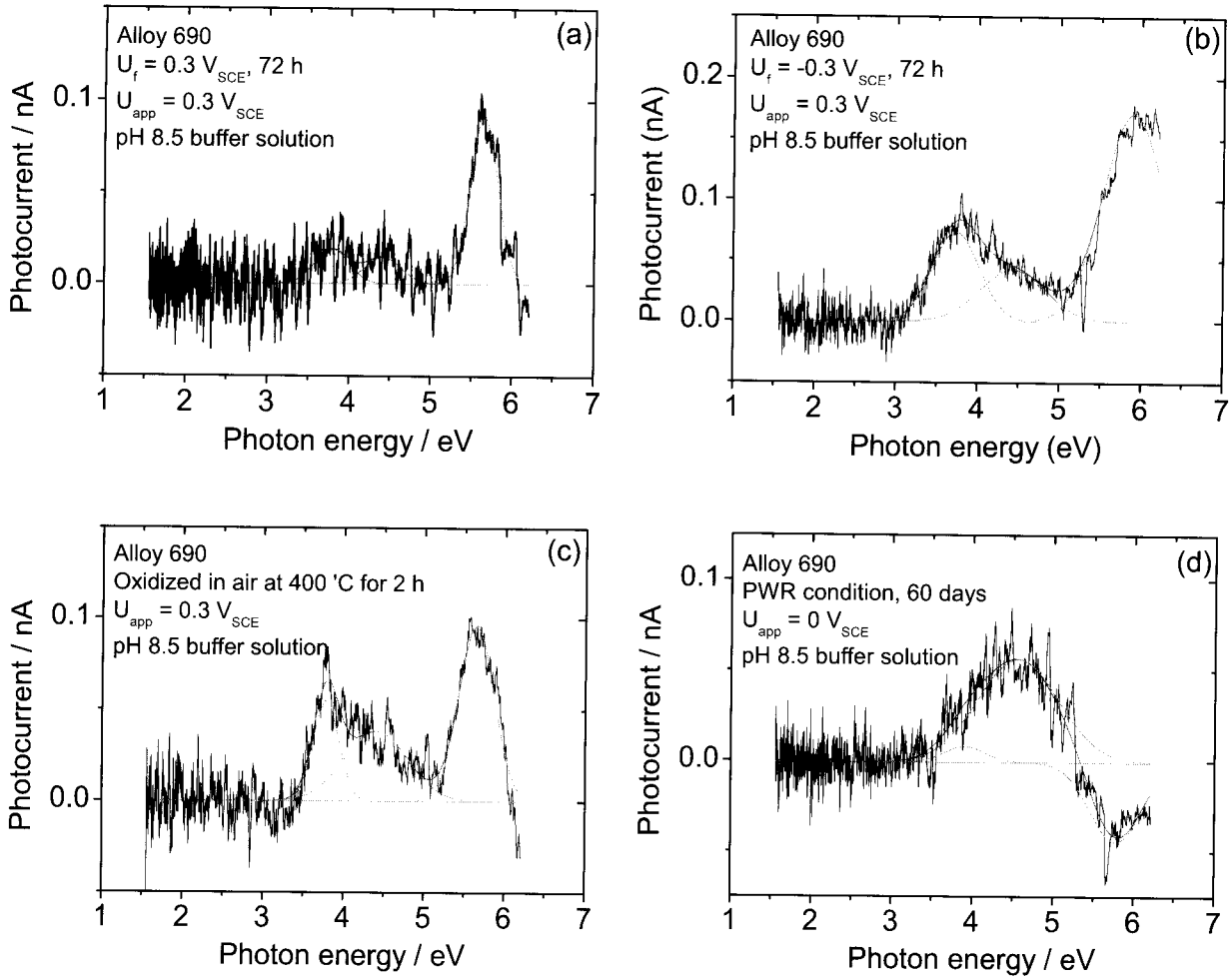

Fig. 5. Photocurrent spectra for the passive films formed on Alloy 690 (a) at 0.3 V_{SCE}, (b) at -0.3 V_{SCE} in pH 8.5 buffer solution at ambient temperature, (c) in air at 400 ℃, and (d) in PWR condition, measured at selected applied potentials to show all of the photocurrent spectral components generated from the films.

photocurrent spectrum are affected by the film formation conditions and the film formation time in solution as well (described elsewhere[17]).

The photocurrent spectra in Figs. 4 and 5 suggest the passive films formed on Alloy 690 in various film formation conditions are composed of Cr_2O_3, $Cr(OH)_3$, Fe_2O_3, $Ni(OH)_2$, and NiO, complementing the XPS results.

3.4 Mott-schottky analysis

The type and concentration of point defect in the passive film were examined by Mott-Schottky analysis. From Fig. 6, the Mott-Schottky plots for the passive films formed on Alloy 690 at various film formation conditions exhibited positive slopes at potentials above -0.5 V_{SCE} but the slope was negative or nearly zero at potentials below -0.5 V_{SCE}. These behaviors are similar to that of the passive films formed on stainless steel and Fe[19] as shown in Fig. 7. The flat band potential of the passive film of Alloy

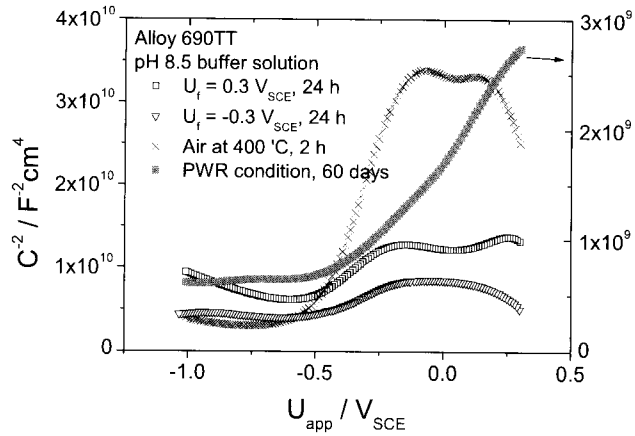

Fig. 6. Mott-Schottky plots for the passive films formed on Alloy 690 in pH 8.5 buffer solution at ambient temperature, in air at 400 ℃, and in PWR condition. Capacitance was measured at 1 kHz with decreasing applied potential at the scan rate of 1 mV/s.

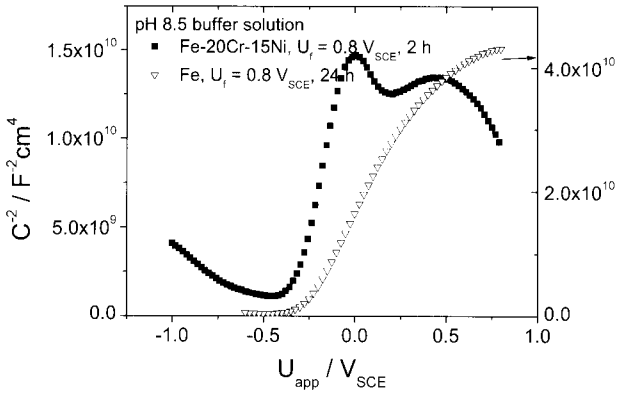

Fig. 7. Mott-Schottky for the passive films formed on Fe-20Cr-15Ni[18] and Fe[19] at 0.8 V_{SCE} in pH 8.5 buffer solution, presented for comparison with those for the passive films on Alloy 690.

690 was determined to be -0.5 ~ -1 V_{SCE} by extrapolating the linear regions with positive slope in Fig. 4, being close to those (-0.3 ~ -0.5 V_{SCE}) for the films of stainless steel and Fe[19] (Fig. 7). Therefore, the capacitance of the passive film is considered to be largely affected by Fe oxide rather than Ni or Cr compounds, although Ni and Cr dominate the chemical composition of the film (Fig. 2).

The negative slope observed at low potentials is known to be caused by p-type Cr_2O_3, becoming steeper by increasing Cr content in Fe-Cr alloys.[20] The passive film formed in PWR condition did not show the negative slope due presumably to the relatively low Cr concentration and high Fe concentration in the film as shown in the concentration profile in Fig. 2. For the films formed at 0.3 V_{SCE} in pH 8.5 buffer solution and in air at 400 ℃, the change in slope at about 0.1 V_{SCE} is explained by the presence of deep donor attributed to Cr^{6+} ion.[21] The XPS spectra shown in Fig. 3 confirm this suggestion in that the second slope appeared only in the Mott-Schottky plots for the passive film containing Cr^{6+}.

The density of shallow donor (N_D), i.e., concentration of oxygen vacancy,[8] was estimated to be 1.2×10^{21} ~ 4.6×10^{21} cm^{-3} by Eq. 1 with ε of 12,[22] and was higher in the passive films with lower Cr content (Fig. 2), suggesting that Cr reduces the concentration of oxygen vacancy in the passive film.

$$\frac{1}{C_{SC}^{2}} = \left(\frac{2}{\varepsilon\varepsilon_0 e N_d}\right)\left(U - U_{fb} - \frac{kT}{e}\right) \quad (1)$$

3.5 The correlation between the chemical composition and defect density

Cr content in Ni-based alloys is considered to be the key factor in determining corrosion resistance.[4-6] Acknowledging that the growth and breakdown of passive film is controlled by transport of point defects[8-9] through the film, the enrichment of Cr in the film should essentially involve certain influences on the defect property of the passive film. Therefore, we need to quantitatively investigate the correlation between the Cr content and the concentration of point defect, i.e., oxygen vacancy for the passive film of Alloy 690.

Semiconducting properties of the space charge layer at the film/solution interface are analyzed by Mott-Schottky plots, from which useful information on the type and concentration of point defects are explored.[23] In this concept, we compared the donor density with the average composition of the space charge layer (Fig. 6). The average chemical composition in the space charge layer was determined from the depth concentration profile in Fig. 2 with the thickness of the space charge layer at -0.3 V_{SCE}, at which all the Mott-Schottky plots showed positive slope. The thickness was calculated from the capacitance by following equation and summarized in Table 3;

$$W = \frac{\varepsilon\varepsilon_0}{C} \quad (2)$$

where W is the thickness of space charge layer.

From Fig. 8, increasing Cr content in the passive film reduced the donor density. This result proposes a possible

Table 3. Thickness of the space charge region for the passive film formed on Alloy 690 at various film formation conditions.

Film formation condition	U_f = 0.3 V_{SCE}	U_f = -0.3 V_{SCE}	air at 400 ℃	PWR condition
W / nm	1.11	0.86	1.53	0.33

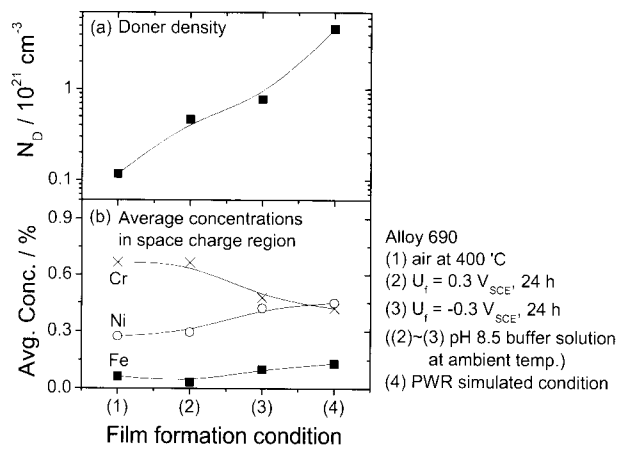

Fig. 8. Effects of film formation condition on (a) the donor density and (b) chemical composition of the passive film of Alloy 690.

explanation for the beneficial effects of Cr on the protectiveness of the passive film as reduction of the oxygen vacancy concentration. In addition, Cr^{6-} in the passive films formed at 0.3 V_{SCE} in buffer solution and in air at 400 ℃ may also contribute to reduction of oxygen vacancy in that incorporation of Cr^{6+} causes excess positive charge and hence could suppress generation of positive charge with oxygen vacancy (V_O^{2+}).

4. Conclusions

The effects of film formation condition on the chemical composition and the semiconducting properties were examined for the passive film formed on Alloy 690 in pH 8.5 buffer solution at ambient temperature, in air at 400 ℃, and in PWR simulated autoclave environment. The findings based on using XPS and Mott-Schottky analysis in this study are as follows:

• It was found from XPS analysis and photocurrent spectra that passive film formed on Alloy 690 comprised Cr_2O_3, $Cr(OH)_3$, NiO, $Ni(OH)_3$, and Cr-substituted γ-Fe_2O_3.

• From the depth composition profile, the passive films formed at high potential (0.3 V_{SCE}) in buffer solution and in air at 400 ℃ were highly enriched with Cr in forms of Cr^{3-} and Cr^{6+}, while the films formed at low potential (-0.3 V_{SCE}) in buffer solution and in PWR condition showed relatively low concentration of Cr, mostly in Cr^{3+}.

• Mott-Schottky plots for the passive film on Alloy 690 exhibited positive slopes, confirming that the semiconducting properties of the film is largely controlled by n-type Cr-substituted γ-Fe_2O_3 with donor density of $1.2\times10^{21} \sim 4.6\times10^{21}$ cm^{-3}.

• By comparing the dependence of the donor density and the chemical composition respectively on the film formation condition, it was found that the concentration of point defect, i.e., oxygen vacancy, was reduced with increase in Cr content in the outer region of passive film.

Acknowledgements

The authors gratefully acknowledge the financial support from Korea Electrical Engineering and Science Research Institute, grant No. R-2003-B-537 and Korea Science and Engineering Foundation, grant No. R01-2003-000-10836-0.

References

1. P. Schmuki and H. Bohni, *J. Electrochem. Soc.* **139**, 1908 (1992).
2. M. Da Cunha Belo, B. Rondot, C. Compere, M. F. Montemor, A. M. P. Simões, and M. G. S. Ferreira, *Corros. Sci.* **40**, 481 (1998).
3. N. Sato, *Corros. Sci.* **42**, 1957 (2000).
4. D. Marijan, M. Vuković, P. Pervan, and M. Milun, J. Appl. Electrochem., **28**, 96 (1998).
5. H. P. Kim, S. S. Hwang, Y. S. Lim, I. H. Kuk, and J. S. Kim, *Key Eng. Mater.* **183-187**, 707 (2000).
6. J. Daret, Proceeding of the 2001 ICG-EAC metting, Kyongju, Korea, April, 2001, p. 23.
7. D. H. Hur, *Corrosion*, **59**, 203 (2003).
8. C. Y. Chao, L. F. Lin, and D. D. Macdonald, *J. Electrochem. Soc.* **128**, 1187 (1981).
9. S. J. Ahn, H. S. Kwon, and D. D. Macdonald, *J. Electrochem. Soc.* **152**, B482 (2005).
10. E. A. Cho, H. S. Kwon, and D. D. Macdonald, *Electrochim. Acta,* **47**, 1661 (2002).
11. H. J. Jang, C. J. Park, and H. S. Kwon, *Electrochim. Acta,* **50**, 3503 (2005).
12. J. F. Moulder, W. F. Stickel, P. E. Sobol, and K. D. Bomben, Handbook of X-ray Photoelectron Spectroscopy, Physical Electronics (1995).
13. J. S. Kim, E. A. Cho, and H. S. Kwon, *Electrochim. Acta,* **47**, 415 (2001).
14. J. S. Kim, E. A. Cho, and H. S. Kwon, *Corros. Sci.* **43**, 1403 (2001).
15. S. J. Lee, E. A. Cho, S. J. Ahn, and H. S. Kwon, *Electrochim. Acta*, **46**, 2605 (2001).
16. U. Stimming, *Electrochim. Acta,* **31**, 415 (1986).
17. H. J. Jang, Ph. D. Thesis, KAIST (2006).
18. H. J. Jang and H. S. Kwon, *Electroanal. Chem.*, **590**, 120 (2006).
19. S. J. Ahn and H. S. Kwon, *Electroanal. Chem.* **579**, 311 (2005).
20. N. E. Hakiki, S. Boudin, B. Rondot, and M. Da Cunha Belo, *Corr. Sci.*, **37**, 1809 (1998).
21. E. A. Cho, Ph. D. Thesis, KAIST (2002).
22. M. Da Cunha Belo, N. E. Hakii, and M. G. S. Ferreira, *Electrochim. Acta*, **44**, 2473 (1999).
23. G. Goodlet, S. Faty, S. Cardoso, P. P. Freitas, A. M. P. Simões, M. G. S. Ferreira, and M. Da Cunha Belo, *Corros. Sci.* **46**, 1479 (2004).
24. A. C. Lloyd, D. W. Shoesmith, N. S. McIntyre, and J. J. Noël, *J. Electrochem. Soc.*, **150**, B120 (2003).